

## LOW-ERROR EQUAL-AREA MAP PROJECTIONS FOR GLOBAL MAPPING OF THE TERRESTRIAL ENVIRONMENT

CANTERS F., CROLS T.

Vrije Universiteit Brussel, BRUSSEL, BELGIUM

### ABSTRACT

Many applications at the global or continental scale involve area-based analysis. Global data sets are therefore often mapped in equal-area reference systems. Use of standard equal-area map projections for global mapping inevitably leads to substantial scale distortion and angular distortion in peripheral areas. In this paper an equal-area polynomial transformation is applied to produce low-error pseudocylindrical equal-area projections for global terrestrial applications, using both non-interrupted and interrupted map designs. Results show that for continuous representations of the Earth's surface average distortion of scale can be substantially reduced, depending on the equal-area projection one starts from. For interrupted projections, overall improvement in scale distortion is limited, yet distortion patterns are better adapted to the distribution of the continental area within each zone of the graticule, leading to less extreme distortion in the periphery, especially in zones with high longitudinal extent.

### BACKGROUND AND OBJECTIVES

Many applications at the global or continental scale, e.g. estimation of the extent of biomes for environmental monitoring and modelling, involve area-based analysis. Global data sets are therefore often mapped in equal-area reference systems. Use of standard equal-area map projections for global mapping, however, always results in substantial scale distortion and angular distortion in peripheral areas. This may be problematic when typical GIS operations (e.g. measuring of distances, buffering, ...) have to be applied on the data. In the context of remote sensing, Usery *et al.* (2003) showed how resampling of remote sensing data sets, when transforming the data into different global reference systems, may lead to substantial loss of spectral information depending on the type of map projection that is used. This also stresses the importance of choosing a proper map projection for global mapping applications, not introducing excessive stretching or compression in some parts of the graticule.

When terrestrial or oceanic data need to be mapped, interruption of map projections can be a very effective way to reduce distortion. Many interrupted map projections have been proposed (Dahlberg, 1962), from simple double hemispheric projections to more complex designs with transpolar continuity, such as Bartholomew's Regional Projection (Bartholomew, 1942) or Berghaus' star projection (see Snyder, 1993, p. 139), or with continuity along the equatorial axis, like Goode's interrupted pseudocylindrical projections (Goode, 1917; Goode, 1925). The latter type, with different parts of the northern and southern hemisphere represented in relation to their own central meridian became a very popular scheme for interrupted map design in the twentieth century and is still very much in use today. By restricting the longitudinal extent within each zone of the map, distortion along the outer meridians, typical of non-interrupted map projections, is reduced.

The best known example of an interrupted map projection with continuity along the equator is Goode's Homolosine projection (Goode, 1925), which is often used for global mapping purposes. The projection consists of six asymmetrically defined zones (2 in the northern and 4 in the southern hemisphere) and is obtained by joining the sinusoidal and the Mollweide projection along the latitude of equal scale of both projections (approximately  $40^{\circ}44'11.98''$ ), using the sinusoidal for the low and the Mollweide for the high latitudes. By fusion of both projections the relatively strong north-south stretching of the Mollweide in the low latitudes and the sharp convergence of the meridians of the sinusoidal projection in the high latitudes is avoided. Yet in spite of its favourable distortion characteristics compared to non-interrupted equal-area graticules, the projection still shows substantial scale distortion near the edges of its zones, especially in the Eurasian zone with its relatively high longitudinal extent.

To reduce distortion in equal-area map projections, error-reducing transformations based on polynomials may be applied, transforming a standard equal-area map projection into a new equal-area projection with less scale distortion, with a distortion pattern better adapted to the overall shape of the area to be mapped (Canters, 2002). In this study, polynomial transformation will be applied to non-interrupted as well as interrupted equal-area map projections to produce low-error equal-area projections, minimising distortion over the terrestrial area. Low-error graticules will be compared to their parent projections, both in terms of

overall distortion, as well as by examining local distortion characteristics in peripheral parts of the graticule.

## APPROACH AND METHODS

### *Error-reducing equal-area transformations*

The use of error-reducing transformations was first proposed for conformal mapping using complex-algebra polynomials (Driencourt and Laborde, 1932), and applied for producing low-error conformal map projections for continental areas (Miller, 1953) as well as for individual countries (Reilly, 1973; Snyder, 1984; Gonzalez-Lopez, 1995), with distortion patterns adapted to the shape of the area to be mapped. A simple affine transformation to modify the distortion pattern of an equal-area projection was proposed by Tobler in 1974 (Tobler, 1974). Canters (1991) generalised Tobler's approach by proposing two polynomial-type mapping functions to transform standard equal-area projections into equal-area graticules with less overall scale distortion:

$$X = f_1(x) \quad Y = \frac{y}{dX/dx} \quad (1)$$

and

$$X = \frac{x}{dY/dy} \quad Y = f_2(y) \quad (2)$$

with  $x, y$  the coordinates of the original projection, and  $X, Y$  the coordinates of the transformed projection and with

$$f_1(x) = \sum_{i=1}^n C_i x^i \quad f_2(y) = \sum_{i=1}^n C'_i y^i \quad (3)$$

Transformation (1) is symmetric about the  $X$ -axis and preserves the proportional scaling along the  $y$ -axis of the original projection. Straight lines parallel to the  $y$ -axis remain straight. Transformation (2) is symmetric about the  $Y$ -axis and preserves the proportional scaling along the  $x$ -axis. Straight parallels in the original graticule remain straight. Consecutive application of both transformations provides a flexible means to transform standard equal-area projections into new, low-error graticules. Canters (2002, 2007) applied both transformations, using fifth-order polynomials, to produce low-error equal-area projections for the EU with distortion patterns closely adapted to the irregular shape of the European Union.

This paper focuses on the development of low-error pseudocylindrical projections for global mapping. Hence use was made of transformation (2), as it preserves the straightness of the parallels of the parent projection. Because transformation (2) preserves the proportional scaling along the Equator as well, it can also be applied to transform interrupted map projections consisting of a set of longitudinal zones touching along a straight equatorial axis without disrupting the continuity of the meridians where they cross the Equator. Using a fifth order polynomial and imposing symmetry about the Equator, transformation (2) becomes:

$$X = x / (C'_1 + 3C'_3 y^2 + 5C'_5 y^4) \quad (4)$$

$$Y = C'_1 y + C'_3 y^3 + C'_5 y^5$$

This 3-parameter transformation was used for developing the various continuous and interrupted low-error equal-area graticules proposed in this paper.

### *Measuring distortion on equal-area map projections*

To quantify distortion for the area of interest (in this case the terrestrial area) a suitable distortion metric needs to be defined. Optimal coefficient values for the equal-area transformation that is applied will be those that minimise the chosen distortion metric. The traditional way of estimating overall distortion in a map projection is to subdivide the area to be mapped into a large number of small plots, and to calculate the value of a local distortion measure for each plot. Overall distortion is then obtained as an area-weighted average of local distortion values. For equal-area projections maximum angular distortion can be considered a suitable metric. Maximum angular distortion for a particular location can be calculated from the principal scale factors  $a$  and  $b$ , representing the scale distortion in the direction of the axes of Tissot's indicatrix, and is given by:

$$2\Omega = 2 \operatorname{asin} \frac{a-b}{a+b} \quad (5)$$

Average angular distortion over an area of interest is then calculated as:

$$E_{an} = \frac{1}{S} \sum_{i=1}^k 2 a \sin \frac{a_i - b_i}{a_i + b_i} P_i \cos \phi_i \quad (6)$$

with

$$S = \sum_{i=1}^k P_i \cos \phi_i \quad (7)$$

and with  $a_i$  and  $b_i$  the principal scale factors in point  $i$ ,  $P_i = 1$  if the position is located on continental area and  $P_i = 0$  if it is not. In this study distortion was calculated for every  $2.5^\circ$  longitude and latitude.

As an alternative for calculating distortion at the infinitesimal scale, one can also calculate the distortion of finite-sized distances randomly generated over the area to be mapped, and use the average distortion of all distances as an overall measure of distortion (Gilbert, 1974; Peters, 1975; Albinus, 1981; Canters, 1989). This technique has the advantage that it emphasizes the cumulative effect of scale distortion over finite distances and in different directions. In this study both maximum angular distortion and finite scale distortion were calculated. To characterise finite scale distortion the following distortion measure was used:

$$e_{s,i} = \frac{|s_i - s'_i|}{|s_i + s'_i|} \quad (8)$$

with  $s_i$  the distance between two positions on the globe, and  $s'_i$  the corresponding distance on the map. Short and large distances are equally treated in the calculation of this relative distortion measure. Enlargements and reductions by the same factor lead to the same distortion value. After calculating finite scale distortion for a large number of distances, an average scale factor (defining the average distortion of distances of unit length) can be obtained as follows:

$$K_s = \frac{1}{m} \sum_{i=1}^m \frac{1 + e_{s,i}}{1 - e_{s,i}} \quad (9)$$

with  $m$  the number of distances. Initial experiments showed that the use of 50000 distances leads to stable results. When working with interrupted projections, only distances defined within the same zone of the graticule can be used.

### Choice of parent projections

Two well-known pseudocylindrical projections with a clearly different appearance, the sinusoidal projection and the Mollweide projection, were chosen as parent projections for the derivation of low-error equal-area graticules. The sinusoidal projection, with equally spaced parallels of correct length and sharply converging meridians, is characterised by a high angular distortion in the high latitudes (figure 1). The Mollweide projection, with its ellipsoidal meridians and decreasing distance between the parallels from the equator towards the poles shows a strong N-S stretching in the low latitudes (figure 2).

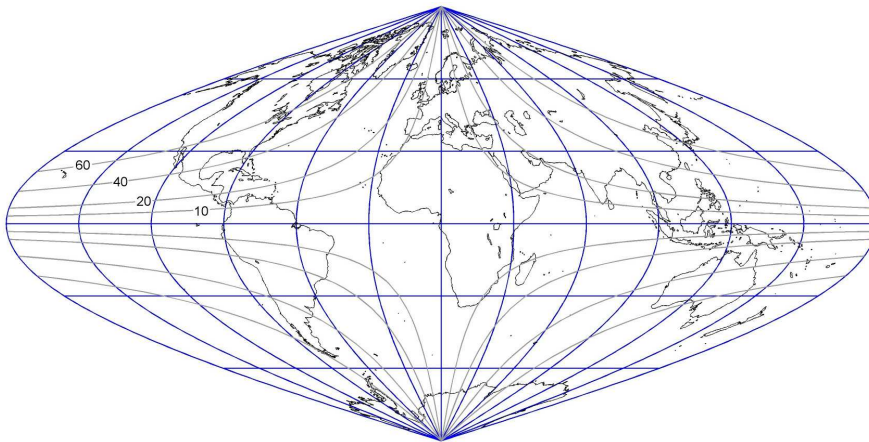


Figure 1: Sinusoidal projection with lines of equal maximum angular distortion ( $^\circ$ )

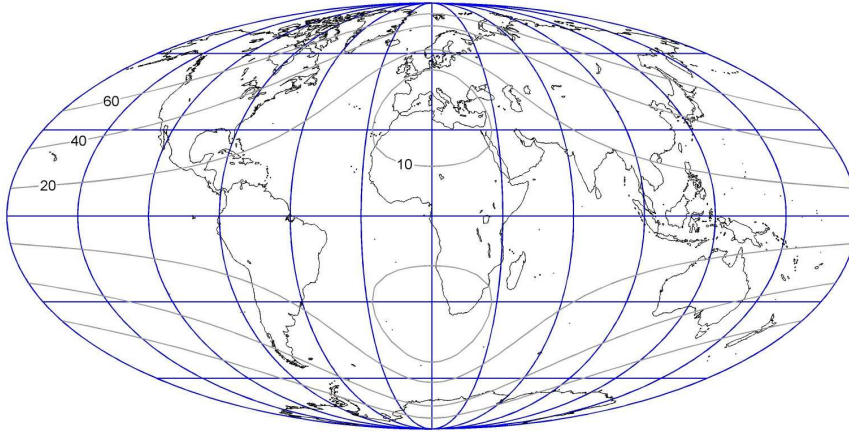


Figure 2: Mollweide projection with lines of equal maximum angular distortion (°)

Starting from the sinusoidal projection and the Mollweide projection, non-interrupted low-error equal-area projections were developed by applying the 3-parameter transformation described above (see equation (4)), using both maximum angular distortion and average finite scale distortion ( $= K_s - 1$ ) as criteria for optimisation. In all four cases the central meridian was chosen at  $10^\circ\text{E}$ . This puts Africa in the centre of the map and does not split Eastern Siberia near the Bering Sea, as is the case when the central meridian is chosen at  $0^\circ$ .

Interrupted versions of the sinusoidal projection and the Mollweide projection with five separate zones were used as starting point for developing optimised versions of these two projections, using average finite scale distortion for optimisation. The interruption scheme that was chosen comprises two zones in the northern hemisphere: North America ( $\lambda_0 = 105^\circ\text{W}$ ) and Eurasia ( $\lambda_0 = 60^\circ\text{E}$ ), with an interruption between both zones defined at  $30^\circ\text{W}$ ; and three zones in the southern hemisphere: South America ( $\lambda_0 = 60^\circ\text{W}$ ), Africa ( $\lambda_0 = 25^\circ\text{E}$ ) and Australia ( $\lambda_0 = 135^\circ\text{E}$ ), with interruptions at  $30^\circ\text{W}$  and  $60^\circ\text{E}$  (figure 5).

For interrupted projections, experiments with global as well as zonal optimisation were done. Global optimisation uses the same polynomial coefficients for the transformation of all continental zones, while zonal optimisation produces zone-specific sets of coefficients. However, to maintain continuity across the equator, zonal coefficients cannot be produced for each of the five zones separately. Zonal coefficients could be derived only for the two American zones as a whole (west of  $30^\circ\text{W}$ ), and for the three other continental zones together (east of  $30^\circ\text{W}$ ).

Previous work on map projection optimisation demonstrated the negative impact of including Antarctica as part of the area to be optimised on the representation of the terrestrial area as a whole (Canters, 2002). For that reason the Antarctic continent was not included as part of the terrestrial area in the experiments carried out in this study.

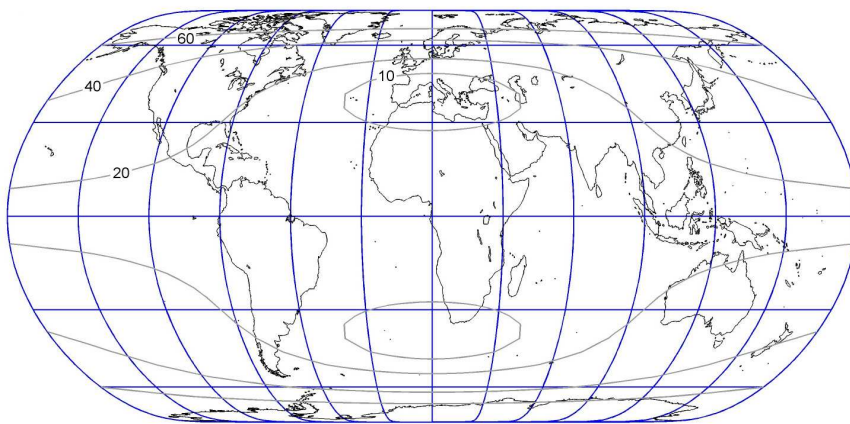
## RESULTS AND DISCUSSION

Table 1 shows average distortion values for non-interrupted graticules for both parent projections (sinusoidal and Mollweide) and for four low-error projections obtained by transforming each parent projection, using either finite scale distortion or maximum angular distortion as a criterion for optimisation. Results demonstrate that for the sinusoidal projection the average distortion of distance is reduced by 29% when applying the 3-parameter equal-area transformation, using distortion of finite distance as a criterion for optimisation. For the Mollweide projection, which already has a substantially lower finite scale distortion than the sinusoidal projection in its original form, the reduction of scale distortion obtained is less. However, distortion values for both low-error graticules are of the same order of magnitude. Optimising the sinusoidal and the Mollweide projection, using maximum angular distortion as a criterion for error minimisation, also produces two graticules with similar overall distortion values (an average angular distortion of  $24^\circ$  against  $35^\circ$  and  $29^\circ$  for the original sinusoidal and the original Mollweide projection respectively).

Table 1: Average finite scale distortion  $(K_s - 1) \times 100$  (%) and average maximum angular distortion  $E_{am}$  for non-interrupted equal-area projections, before and after optimisation. Optimised distortion values are marked in grey.

	$(K_S - 1) \times 100$ (%)	$E_{an}$
Sinusoidal projection (standard)	26.32	34° 80
→ Minimum finite scale distortion	18.65	25° 65
→ Minimum angular distortion	20.47	24° 03
Mollweide projection (standard)	21.15	29° 29
→ Minimum finite scale distortion	18.53	25° 92
→ Minimum angular distortion	20.27	24° 20

Compared to the original sinusoidal projection (figure 1), the meridians of the optimised version of the graticule, obtained by minimising finite scale distortion, are shaped in such a way that the projection seems to have a pole line (figure 3), although this is not really the case (all meridians converge in one point). By creating a virtual pole line, the skewness of the meridians in the high latitudes so characteristic of the original projection is avoided and the overall distortion of finite distances is reduced, leading to a graticule with a more balanced distortion pattern.



*Figure 3: Low-error transformation of the sinusoidal projection (minimum distortion of finite distances) with lines of equal maximum angular distortion (°)*

The other three optimised graticules (not all shown here) feature a virtual pole line as well. When minimising angular distortion instead of distance distortion the pole line approximates the length of the equator, leading to graticules that show some resemblance to cylindrical projections, although meridians are still slightly curved (figure 4). Because of the less balanced distortion patterns obtained when minimising angular distortion, further experiments in this study were all based on minimising the distortion of finite distances.

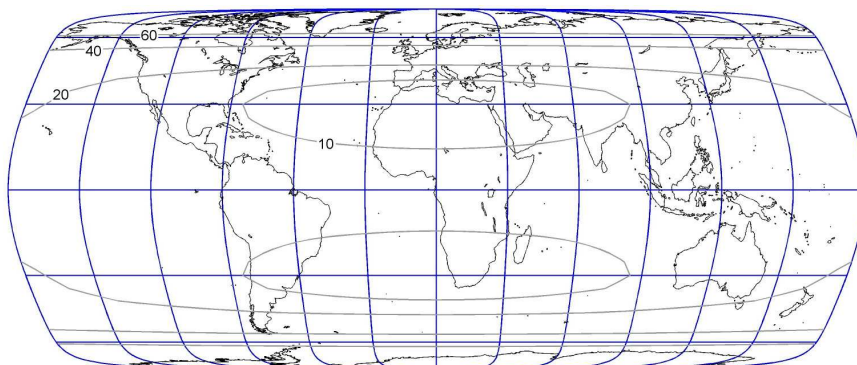


*Figure 4: Low-error transformation of the Mollweide projection (minimum distortion of angles) with lines of equal maximum angular distortion (°)*

Interrupting the sinusoidal and Mollweide projection, using 5 longitudinal zones, leads to a strong reduction of overall finite scale distortion and angular distortion (table 2), compared to a continuous representation of the Earth's surface using these two projections (table 1). Yet also for interrupted projections distortion shows up in the periphery, especially in the Eurasian zone with its high longitudinal

extent (figure 5). Transformation of the interrupted sinusoidal and Mollweide projection, using finite scale distortion as a criterion for error reduction, produces graticules with average distortion values only slightly lower than for the two parent projections, yet with a clear improvement in the representation of those areas that have the largest distortion in the original projection, more in particular Europe and Northeast Asia (figure 6). Starting from the sinusoidal or the Mollweide projection produces nearly identical graticules, with the same error distribution.

*Table 2. Average finite scale distortion  $(K_S - 1) \times 100$  (%) and average maximum angular distortion  $E_{an}$  for interrupted equal-area projections, before and after optimisation. Optimised distortion values are marked in grey. Distortion values for Goode's Homolosine projection are included for comparison.*

	$(K_S - 1) \times 100$ (%)	$E_{an}$
Interrupted Goode Homolosine projection (5 zones)	9.20	15° 87
Interrupted sinusoidal projection (5 zones)	9.06	14° 96
→ Global optimisation	8.72	14° 67
→ Zonal optimisation	8.43	14° 25
Interrupted Mollweide projection (5 zones)	9.86	16° 92
→ Global optimisation	8.69	14° 54
→ Zonal optimisation	8.47	14° 29

Applying the error-reducing transformation separately on the 3 eastern and the 2 western zones leads to an additional (although comparatively small) reduction of finite scale distortion, with mean angular distortion values also slightly decreasing. Coefficients values for both transformations are quite different, the graticule being adapted to the distribution of the continents in the two parts (figure 7). The distortion pattern is slightly more balanced, with even lower distortion values at the extremities of the Eurasian zone compared to the global optimisation result.

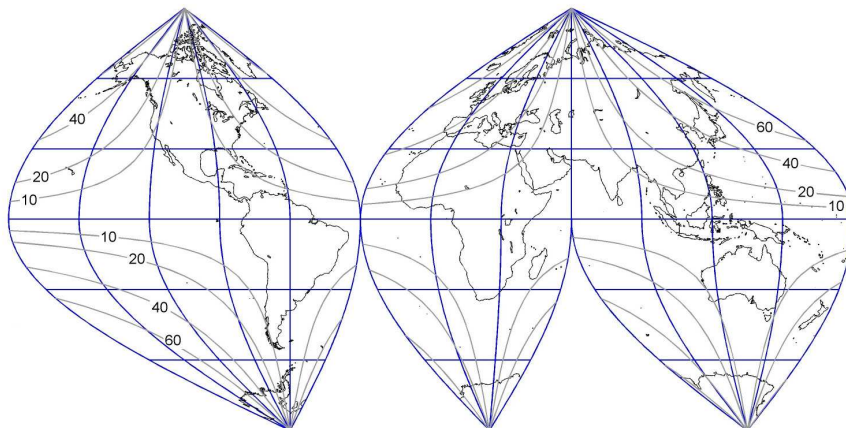


*Figure 5: Interrupted sinusoidal projection with lines of equal maximum angular distortion (°)*

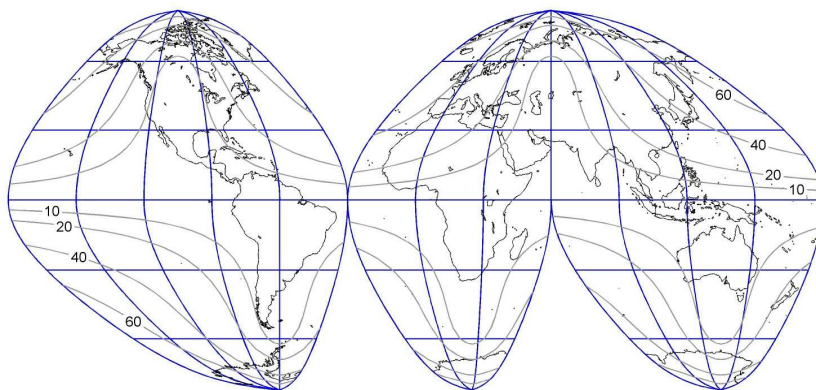


*Figure 6: Low-error global transformation of the interrupted sinusoidal projection (minimum distortion of finite distances) with lines of equal maximum angular distortion (°)*

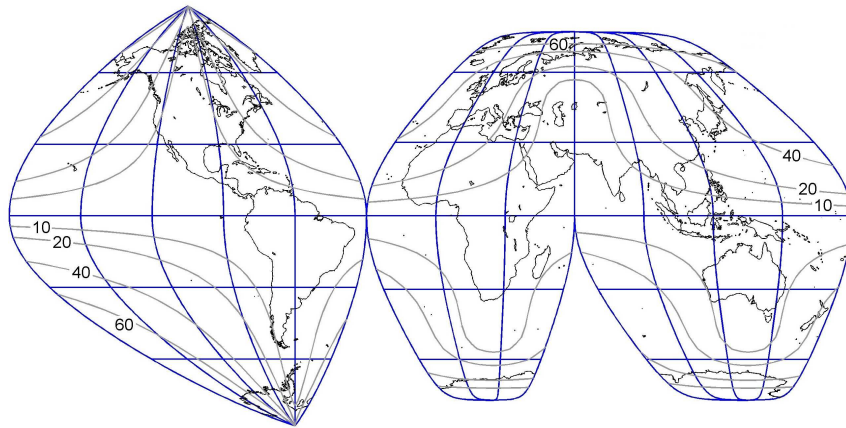


Figure 7: Low-error zonal transformation of the interrupted sinusoidal projection (minimum distortion of finite distances) with lines of equal maximum angular distortion ( $^{\circ}$ )

## CONCLUSION

Global mapping of the Earth's surface in standard equal-area projections typically results in substantial scale distortion and angular distortion in peripheral areas. By applying a simple 3-parameter transformation of the polynomial type and optimising its parameter values based on a minimum-error criterion, a substantial reduction of distortion may be obtained, without loss of the equal-area property. Starting from the sinusoidal and the Mollweide projection, the graticule of both projections is drastically transformed through the introduction of a virtual pole line, leading to a more balanced distortion pattern, better adapted to the distribution of the terrestrial area as a whole. Applied to interrupted versions of the two parent projections, the transformation results in more favourable distortion characteristics for those areas that have the largest distortion in the original graticules, more specifically Europe and Northeast Asia. Zonal optimisation of transformation parameters generates graticules with even more balanced distortion patterns, better adapted to the distribution of the terrestrial area within each zone, and thus better suited as equal-area reference systems for global terrestrial applications than standard map projection solutions.

## REFERENCES

- Albinus, H.-J., 1981. Anmerkungen und Kritik zur Entfernungsverzerrung, *Kartographische Nachrichten*, 31, 179-183.
- Bartholomew, J., 1942. *The Citizen's Atlas of the World*, Edinburgh: John Bartholomew & Son.
- Canter, F., 1989. New projections for world maps, a quantitative-perceptive approach, *Cartographica*, 26, 53-71.
- Canter, F., 1991. Map projections in a GIS environment, in Rybczuk, K. and Blakemore, M. (Eds.), *Mapping the Nations, Proceedings of the 15th Conference of the International Cartographic Association*, Bournemouth, Vol. 2, 595-604.
- Canter, F., 2002. Small-scale Map Projection Design, in Fisher, P. and Raper, J. (Eds.), *Research Monographs in Geographical Information Systems*, London and New York: Taylor & Francis.
- Canter, F., 2007. Low-error map projections for pan-European equal-area mapping, *Proceedings of the 23th International Cartographic Conference*, August 4-10, Moscow, Russia, CD-ROM.
- Dahlberg, R.E., 1962. Evolution of Interrupted Map Projections, *International Yearbook of Cartography*, 2, 36-54.
- Driencourt, L. and Laborde, J., 1932. *Traité des Projections des Cartes Géographiques à l'Usage des Cartographes et des Géodésiens*, 4 fascicules, Paris : Hermann et Cie.
- Gilbert, E.N., 1974. Distortion in maps, *Society for Industrial and Applied Mathematics Review*, 16, 47-62.
- Gonzalez-Lopez, S., 1995. Conformal map projections by least squares adjustment with conditions between parameters, *Proceedings of the 17th International Cartographic Conference*, Barcelona, 776-780.
- Goode, J.P., 1917. A new idea for a world map: a substitute for Mercator's projection, *Annals of the Association of American Geographers*, 7, 75-76.
- Goode, J.P., 1925. The Homolosine projection, a new device for portraying the Earth's surface entire, *Annals of the Association of American Geographers*, 15, 119-125.
- Miller, O.M., 1953. A new conformal projection for Europe and Asia, *Geographical Review*, 43, 405-409.
- Peters, A.B., 1975. Wie man unsere Weltkarten der Erde ähnlicher machen kann, *Kartographische Nachrichten*, 25, 173-183.

- Reilly, W.I., 1973. A conformal mapping projection with minimum scale error, *Survey Review*, 22, 57-71.
- Snyder, J.P., 1984. A low-error conformal map projection for the 50 States, *American Cartographer*, 11, 27-39.
- Snyder, J.P., 1993, *Flattening the Earth, Two Thousand Years of Map Projections*, Chicago: The University of Chicago Press.
- Tobler, W.R., 1974. Local map projections, *American Cartographer*, 1, 51-62.
- Usery, E.L., Seong, J.C., Steinwand, D.R. and Finn, M.P., 2003. Accurate projection of small-scale raster datasets, *Proceedings of the 21st International Cartographic Conference*, 10-16 Aug 2003, Durban, South Africa.